Hydrogen Bonding Effect on the Poly(ethylene oxide), Phenolic Resin, and Lithium Perchlorate–Based Solid-State Electrolyte

Hsien-Wei Chen, Chang-Hung Jiang, Hew-Der Wu, Feng-Chih Chang

Institute of Applied Chemistry, National Chiao-Tung University, Hsin-Chu, 30043, Taiwan, Republic of China

ABSTRACT: The interaction behavior of solid-state polymer electrolytes composed of poly(ethylene oxide) (PEO)/novolac-type phenolic resin and lithium perchlorate (LiClO$_4$) was investigated in detail by DSC, FTIR, ac impedance, DEA, solid-state NMR, and TGA. The hydrogen bonding between the hydroxyl group of phenolic and ether oxygen of the PEO results in higher basicity of the PEO. The higher basicity of the ether group can dissolve the lithium salts more easily and results in a greater fraction of "free" anions and thus higher ionic conductivity. DEA results demonstrated that addition of the phenolic increases the dielectric constant because of the partially negative charge on the ether group induced by the hydrogen bonding interaction between ether oxygen and the hydroxyl group. The study showed that the blend of PEO(100)/LiClO$_4$(25)/phenolic(15) possesses the highest ionic conductivity (1.5 × 10^{-5} S cm^{-1}) with dimensional stability. © 2003 Wiley Periodicals, Inc. J Appl Polym Sci 91: 1207–1216, 2004

Key words: poly(ethylene oxide) (PEO); resins; hydrogen bonding; ionic conductivity; solid-state structure

INTRODUCTION

Since the original work of Wright and Armand on poly(ethylene oxide) (PEO)/alkali metal salt–based solid polymer electrolytes (SPEs),[1–4] research efforts for improvement of ionic conductivity have become quite active. During the past decade, lithium salt–based electrolytes have been the focus of numerous fundamental and application-oriented studies.[5–10] Most research has focused on the development of high power and high energy density secondary lithium batteries with major concerns directed to performance, safety, and reliability. Applications of lithium batteries in automotive industries, portable devices, and aerospace applications are presently a subject of great interest.

PEO-based polymer electrolytes are still among the most extensively studied polymer ionic conductors because of the beneficial structure in supporting fast ion transport.[7,11–13] Two approaches for achieving high conductivity of PEO-based SPE are the suppression of PEO crystallization to improve the chain mobility and increase of the charge carrier. Chu et al.[18] reported that the addition of phenolic resin can enhance the conductivity because of the reduced PEO crystallinity and lower pseudoactivation energy in lithium transfer of the blend. However, in addition to the hydrogen bonding interaction, the specific interactions between the phenolic resin, PEO, and lithium salts were not discussed. In this study, we attempted to add the novolac phenolic to the PEO/LiClO$_4$ electrolyte system by suppressing PEO crystallization through strong hydrogen bonding interaction between the ether group of PEO and the hydroxyl group of the novolac phenolic. The obtained blend of PEO(100)/LiClO4(25)/phenolic(15) possesses high ionic conductivity of 1.5 × 10^{-5} S cm^{-1} at room temperature and elastic property. Based on IR spectra of OH$^-$ and ClO$_4^-$ vibrations, the increase in conductivity is not only from the increase in amorphous fraction but also from the complicated interaction among PEO, phenolic, and lithium salt. These IR vibrations were used to interpret the complicated interaction mechanism among PEO, phenolic, and the lithium salt. The purpose of this work was to emphasize the effect on the fraction of hydrogen bonding by adding phenolic to provide the PEO/LiClO$_4$/phenolic blend system.

EXPERIMENTAL

Sample preparation

The novolac-type phenolic resin was synthesized and analyzed as described previously.[19] The chemical structure of the novolac-type phenolic resin consists of phenol rings bridge-linked randomly by methylene groups with 19% *ortho–ortho*, 57% *ortho–para*, and 24% *para–para* methylene bridges as identified by solution ^{13}C-NMR. The poly(ethylene oxide) (PEO) with M_n of

Correspondence to: F.-C. Chang (changfc@cc.nctu.edu.tw).

TABLE I
Desired Amount for PEO(100)/Li(25)/Phenolic(x)

Component (wt)	Weight fraction (wt %) for PEO, Li, and phenolic					
	Phenolic concentration (x)					
	0	5	10	15	20	25
PEO (100 g)	80.0%	76.9%	74.1%	71.4%	69.0%	66.7%
Li (25 g)	20.0%	19.2%	18.5%	28.6%	17.2%	16.7%
Phenolic (x g)	0%	3.8%	7.4%	10.7%	13.8%	16.7%

200,000 was obtained from Aldrich (Milwaukee, WI). The lithium perchlorate salt ($LiClO_4$), also obtained from Aldrich, was dried in a vacuum oven at 80°C for 24 h, and then stored in a desiccator before use. The N,N-dimethyl formamide (DMF) was refluxed at a suitable temperature under nitrogen atmosphere before use.

Preparation of solid polymer electrolytes (SPEs)

The PEO/$LiClO_4$/phenolic complexes of different compositions were prepared by dissolving the desired amount of the PEO (Table I), vacuum dried $LiClO_4$ salt, and phenolic in dry DMF. After continuous stirring for 24 h at 60°C, these solutions were maintained at 130°C for 24 h to facilitate solvent removal, and then further dried under vacuum at 80°C for another 3 days. The samples were analyzed by FTIR (carbonyl group, 1700 cm^{-1}) to monitor the residual solvent. All of these complexes were stored in a dry box filled with nitrogen atmosphere to prevent contact with air and moisture.

The phr unit was used as the formulae in this study. For example, PEO(100)/$LiClO_4$(15) means PEO is nearly 87 wt %; however, the $LiClO_4$ is 13 wt %.

DSC measurements

Thermal property measurements were carried out on a DSC 2010 (TA Instruments, New Castle, DE). The measurements were conducted under a nitrogen atmosphere with a flow rate of about 25 mL min^{-1} and the instrument was calibrated with an indium standard. All samples were annealed for 10 min at 100°C and then rapidly quenched to −100°C and then reheated. A heating rate of 10°C min^{-1} was used in all cases. The glass-transition temperature (T_g) and the crystallization temperature (T_c) were taken as the midpoint of the transition and the minimum of the exothermic peak, respectively, whereas the melt-point temperature (T_m) was taken as the maximum of the endothermic peak.

FTIR measurements

Infrared spectra of composite films were measured using the conventional NaCl disk method. All polymer films were prepared under N_2 atmosphere. The DMF solution of the complex was cast onto a NaCl disk and the solvent was removed under vacuum at 70°C for 48 h. All infrared spectra were obtained with wavenumbers in the range of 4000–400 cm^{-1} with a resolution of 1 cm^{-1} on a Nicolet Avatar 320 FTIR spectrometer (Nicolet Analytical Instruments, Madison, WI).

Conductivity measurements

Ionic conductivity measurements with alternating current (ac) were conducted on an Autolab designed by Eco Chemie in the frequency range from 10 MHz to 10 Hz. The composite film was sandwiched between stainless-steel blocking electrodes (1 cm diameter). The specimen thickness was about 100 μm, and the impedance response was measured over the range from 27 to 80°C.

Dielectric constant analyses

Dielectric constants of composites were measured at different temperatures (from 25 to 40°C) using a TA Instruments DEA 2970 at the frequency of 100 Hz. The specimen thickness varied from 0.2 to 0.3 mm.

TGA measurements

A TG/DTA 200 thermal gravimetric analyzer (Seiko Instruments, Japan) was used to carry out the TGA experiments on the weight loss and thermal decomposition behavior for PEO/$LiClO_4$/phenolic electrolytes in this study. The heating rate was 10°C min^{-1}, from 30 to 600°C, under nitrogen atmosphere.

Solid-state NMR characterizations

High-resolution solid-state ^{7}Li-NMR experiments were carried out on a Bruker DSX-400 spectrometer (Bruker Instruments, Billerica, MA) operating at a resonance frequency of 155.5 MHz. The ^{7}Li magic angle spinning (MAS) spectra were measured with 3 μs, 90° pulse angle, 2-s pulse delay time, 2048 scans, and spinning speed 3 kHz. All NMR spectra were taken at 27°C with proton decoupling and MAS of 10 kHz.
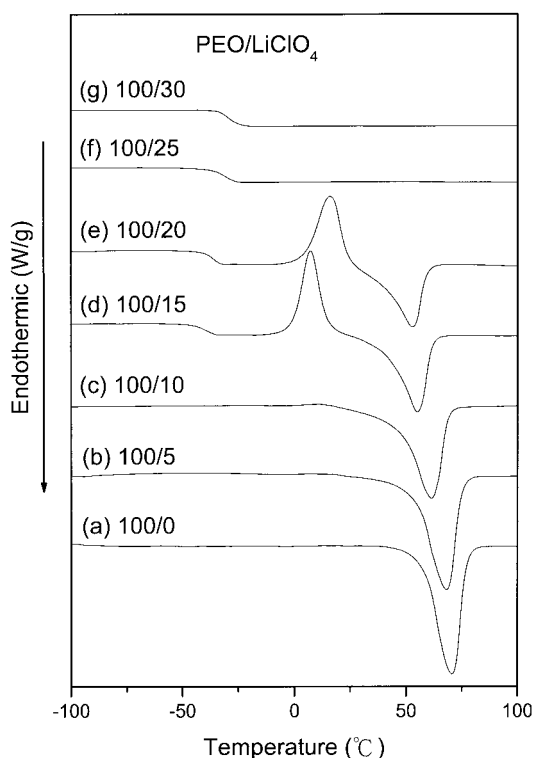
Figure 1 DSC thermograms of the PEO/LiClO$_4$ blends: (a) 100/0; (b) 100/5; (c) 100/10; (d) 100/15; (e) 100/20; (f) 100/25; (g) 100/30.

RESULTS AND DISCUSSION

Thermal properties of solid polymer electrolytes

Figure 1 shows the DSC thermograms of PEO/LiClO$_4$ electrolyte systems with various concentrations of the lithium salt. Thermograms of plain PEO, PEO(100)/

LiClO$_4$(5), and PEO(100)/LiClO$_4$(10) show a single endothermic peak appearing around 70°C, corresponding to the PEO melting peak, an indication of full development of PEO crystallization. By the addition of lithium salts, the melting temperature (T_m) and heat enthalpy of the PEO decreased slightly with increasing LiClO$_4$ content. Mixtures of PEO(100)/LiClO$_4$(15) and PEO(100)/LiClO$_4$(20) show a T_g and both an exothermic and an endothermic peak. As shown in the plot, the mixtures containing 25 and 30 phr LiClO$_4$ give only one T_g, implying that PEO crystallization is suppressed by the presence of LiClO$_4$. Furthermore, the T_g is increased by the increase of LiClO$_4$ content, attributed to the strong interaction of the ethylene oxide group and lithium cation. The appearance of a single T_g in PEO/LiClO$_4$ electrolyte [Fig. 1(f), (g)] strongly suggests that these systems are in a homogeneous single amorphous phase. These thermal properties are consistent with the generally observed behavior of polymer salt electrolytes attributed to the formation of a pseudo-crosslinked system resulting in higher T_g with lower PEO crystalline. Because the higher T_g means lower chain mobility, the polymer chain will be harder to rotate and rearrange. Therefore, the higher T_g results in lower crystallinity. Figure 2 presents the change of T_g for the PEO(100)/LiClO$_4$(25)/phenolic electrolyte system containing various phenolic concentrations. The T_g increases gradually with the increase in phenolic concentration, which increase can be attributed to the strong interhydrogen bonding between hydroxyl groups in the phenolic and ether groups in PEO.[15–20] The single T_g indicates that these PEO/LiClO$_4$/phenolic electrolyte blends form a more miscible and fully amorphous material, which will be good for ionic transference.
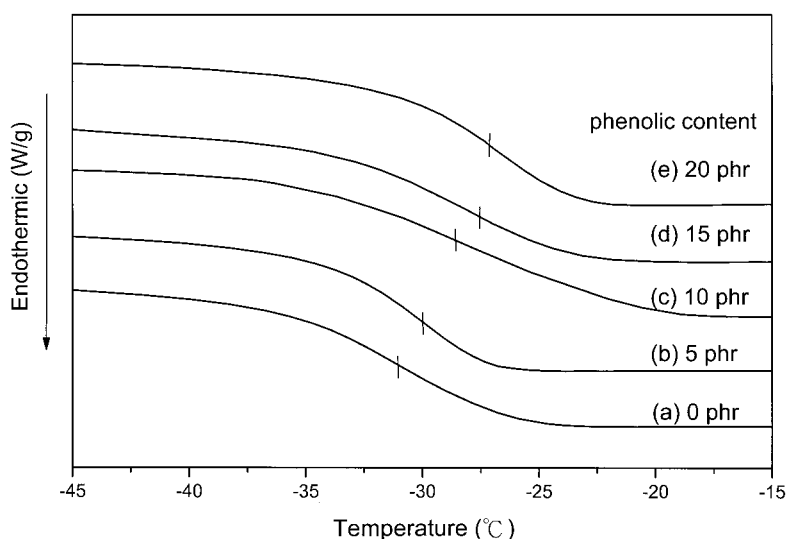

Figure 2 DSC thermograms of PEO/LiClO$_4$/phenolic with various phenolic concentrations: (a) 100/25/0; (b) 100/25/5; (c) 100/25/10; (d) 100/25/15; (e) 100/25/20.
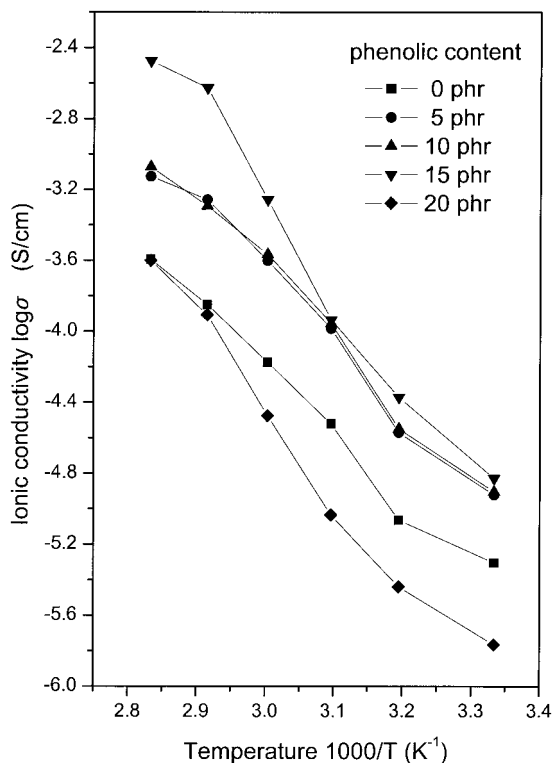
Figure 3 Arrhenius conductivity plots of PEO/LiClO$_4$/phenolic with various phenolic concentrations: (■) 100/25/0; (●) 100/25/5; (▲) 100/25/10; (▼) 100/25/15; (◆) 100/25/20.

Conductivity

Figure 3 presents Arrhenius plots that illustrate the temperature dependency of the ionic conductivity for PEO(100)/LiClO$_4$(25)/phenolic electrolyte composites containing various phenolic concentrations. The conductivity increases with the increase of the phenolic content and attains a maximum value when the phenolic concentration is at 15 phr. Subsequently, the conductivity decreases drastically with further increases of the phenolic content. Figure 4 presents the conductivity isotherms obtained at 40, 60, and 80°C for PEO(100)/LiClO$_4$(25)/phenolic blends as a function of phenolic concentration (phr). A considerable increase in the conductivity is observed by adding a small quantity of the phenolic and the maximum ionic conductivity is achieved at the phenolic concentration of 15 phr. However, the conductivity drastically decreases to even lower than the original value at 20 phr phenolic concentration. At 40°C, the conductivity of PEO(100)/LiClO$_4$(25)/phenolic(15) is about three times higher than that of the plain PEO(100)/LiClO$_4$(25) system. However, the trend of the ionic conductivity is not consistent with the T_g observed in Figure 2. It is interesting to note that specific interactions exist among PEO, LiClO$_4$, and the phenolic.
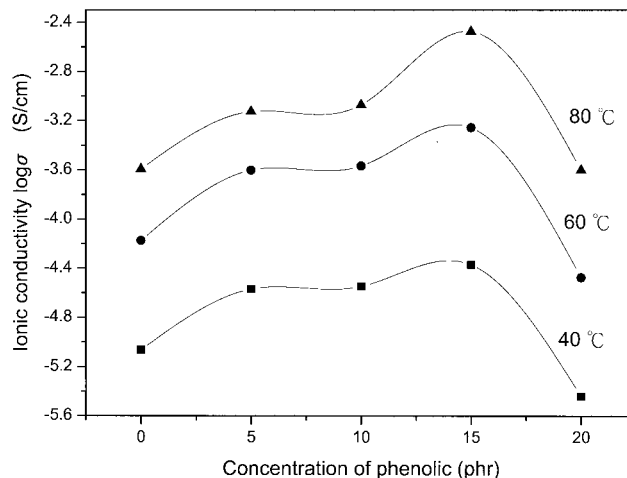

Figure 4 Dependency of ionic conductivity of PEO(100)/LiClO$_4$(25)/phenolic with various phenolic concentrations at the same temperature: (■) 40°C; (●) 60°C; (▲) 80°C.

Infrared spectra

FTIR spectroscopy is a powerful tool for analyzing changes in electrolytic systems, in particular, important information about intermolecular interaction in the PEO/phenolic/LiClO$_4$ electrolyte system. In the PEO-based polymer electrolyte, the Li$^+$ ion tends to associate with the oxygen atom of the PEO, forming a complex, given that the oxygen atom of PEO is a strong electron donor.[24,25] Figure 5 presents the FTIR spectra for the PEO(100)/LiClO$_4$(25)/phenolic with various phenolic concentrations ranging from 4000 to 400 cm^{-1}. The assignments for major bands are listed in Table II.[24–27] As may be observed in Figure 5, the pure PEO has a major peak at 1114 cm^{-1} and two
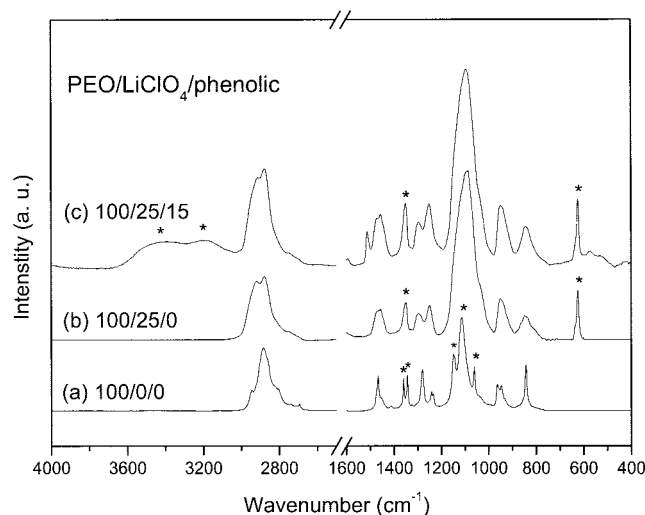

Figure 5 Infrared spectra in the 4000–400 cm^{-1} region of PEO/LiClO$_4$/phenolic blends: (a) 100/0/0; (b) 100/25/0; (c) 100/25/15.

TABLE II
Observed Frequencies and Assignments of Infrared Bands of PEO(100)/LiClO$_4$(25)/Phenolic(15) Blends, in a Cast Film at 27°C, at 1 cm^{-1} Resolution of Experimental Spectra

PEO/LiClO$_4$/phenolic complexes (cm^{-1})	Assignment
3500–3550[a]	Free OH
3200–3600[a]	Hydrogen bonding
2944, 2883, 2805[b]	CH$_2$ or CH stretching
1500, 1600[c]	Phenyl
1460[b]	CH$_2$ bending
1358, 1342[b]	CH$_2$ wagging
1350[b]	Amorphous deformation
1360, 1343[b]	Crystalline deformation
1278, 1241, 1236, 946, 962[b]	CH$_2$ deformation
1060–1150[b]	C—O—C stretching
844[b]	CH$_2$ rocking
600–650, 933, 1025–1100[a]	ClO$_4^-$ anion

[a] Values are for electrolytes.
[b] Values are for PEO.
[c] Values are for phenolic.

minor peaks at 1060 and 1150 cm^{-1}, all of which correspond to the C—O—C stretching motion. The adsorption of the C—O—C region becomes a broad peak with incorporation of 25 phr LiClO$_4$ and the changes of the adsorption could be attributed to the electron surroundings of C—O—C being disturbed by the strong interaction of oxygen atom and lithium cation. In Figure 5(a), one may observe the bands at 1360 and 1343 cm^{-1}, both of which correspond to the crystalline PEO phase. Furthermore, with the blends of PEO(100)/LiClO$_4$(25) and PEO(100)/LiClO$_4$(25)/phenolic(15), the two crystalline split peaks are replaced by a broad band roughly centered at 1350 cm^{-1}, which corresponds to the amorphous regions in PEO. Therefore, blends of PEO(100)/LiClO$_4$(25) and PEO(100)/LiClO$_4$(25)/phenolic(15) are amorphous, which is also consistent with the previous thermograms in Figure 1.

The hydroxyl-stretching region of the PEO/phenolic blends was also examined. Figure 6 shows the infrared spectra in the 3700 to 2900 cm^{-1} region of the pure phenolic and PEO(100)/LiClO$_4$(25)/phenolic blends containing various phenolic contents measured at 25°C. From Figure 6, the pure phenolic polymer is composed of two hydroxyl components: a very broad band, centered at 3340 cm^{-1}, is attributed to the wide distribution of the hydrogen bonded hydroxyl group and a relatively narrow band at 3525 cm^{-1} is caused by the free hydroxyl group. For the blend of PEO(100)/LiClO$_4$(25)/phenolic(5), a shoulder can be found at 3225 cm^{-1}, which can be attributed to the intermolecular hydroxyl–ether bond. By increasing the phenolic content in the PEO(100)/LiClO$_4$(25)/phenolic blend, the intensity of the free hydroxyl group (3525 cm^{-1}) apparently decreases and even disap-

pears. Meanwhile, the broad hydrogen bonded hydroxyl band of the phenolic shifts to a lower frequency and the intensity of the intermolecular hydroxyl–ether bond ($\sim$ 3225 cm^{-1}) increases with increasing phenolic content. The switch of the intramolecular hydroxyl–hydroxyl bond into the intermolecular hydroxyl–ether bond indicates that the hydrogen-bonding interaction between the PEO ether group and the hydroxyl group of phenolic is increased, causing this change. The average strength of the intermolecular interaction can be estimated by the extent of frequency difference ($\Delta\nu$) between the hydrogen-bonded hydroxyl absorption and free hydroxyl absorption, which can be used as a measure of the average strength of the intermolecular interactions.[21–23,28–31] The $\Delta\nu$ increases with increase of the phenolic content, which is higher than the self-associated hydroxyl of the phenolic ($\Delta\nu = 185$ cm^{-1}). Furthermore, the peak at about 3225 cm^{-1} shifts to a lower frequency because of the strong interaction of intermolecular hydrogen bonding, and the strongest interaction can be observed at 15 phr phenolic. However, the peak shifts back at 20 phr phenolic content and this phenomenon can be related to the stronger self-association of higher phenolic content at the expense of the intermolecular hydrogen bonding.[35,36] The above results indicate that strong hydrogen bonding exists between PEO and
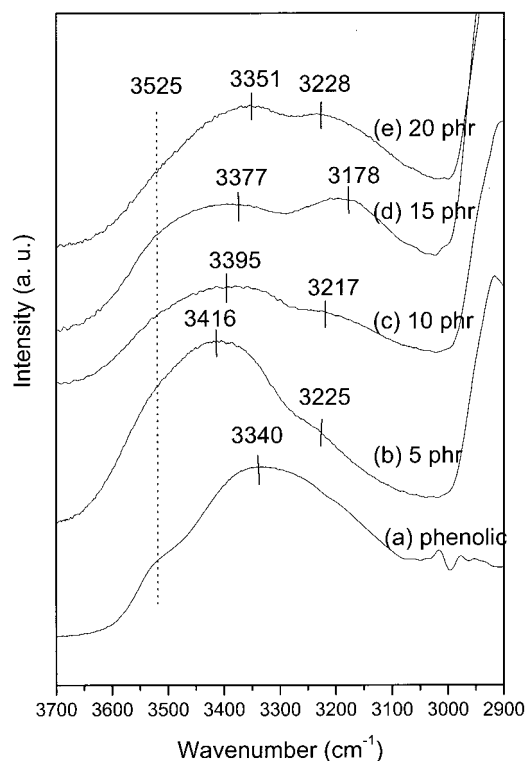

Figure 6 Infrared spectra in the 3700–2900 cm^{-1} region of PEO/LiClO$_4$/phenolic with various phenolic concentrations: (a) pure phenolic; (b) 100/25/5; (c) 100/25/10; (d) 100/25/15; (e) 100/25/20.
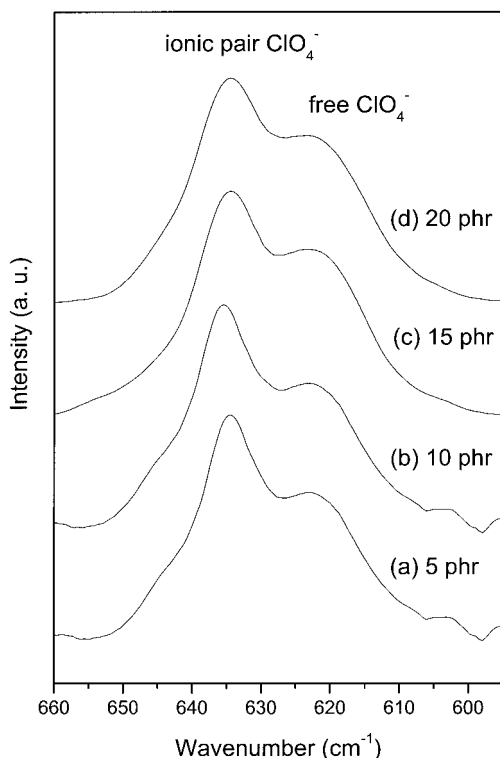
Figure 7 Infrared spectra in the 660–600 cm^{-1} region of LiClO$_4$/phenolic with various phenolic concentrations: (a) 25/5; (b) 25/10; (c) 25/15; (d) 25/20.

phenolic and the strongest intermolecular hydrogen bonding is for the PEO(100)/LiClO$_4$(25)/phenolic(15) blend.

A similar trend is also observed from the ν(ClO$_4^-$) internal mode of the ClO$_4^-$ anion. The characteristic ν(ClO$_4^-$) mode of the lithium perchlorate (LiClO$_4$) is sensitive to the change of the local anionic environment.[14,25–27] According to previously reported studies,[32–34] the component observed at about 624 cm^{-1} was assigned to the "free" anion, which does not interact directly with the lithium cation. Components at about 635 cm^{-1} have been attributed to contact ion pairs. To clarify the interaction between the phenolic and lithium salts, typical infrared spectra in the ν(ClO$_4^-$), ranging from 660 to 595 cm^{-1} at various phenolic concentrations of the LiClO$_4$(25)/phenolic electrolyte system at room temperature, are presented in Figure 7. A strong adsorption band at about 635 cm^{-1} and a relatively weaker peak at about 624 cm^{-1} can be observed. However, no chemical shift or intensity changes were observed for both adsorptions ($\sim$ 635 and $\sim$ 624 cm^{-1}) when varying the phenolic contents. This observation can be interpreted as that the interaction between phenolic and lithium salt is insignificant. In other words, the lithium salt cannot be completely dissolved in the phenolic.

Figure 8 presents the same range of typical infrared spectra in the ν(ClO$_4^-$) spectra at various phenolic

concentrations for PEO(100)/LiClO$_4$(25)/phenolic blends at room temperature. In the absence of the phenolic, a large adsorption band at about 624 cm^{-1} and a shoulder at about 635 cm^{-1} are evident, corresponding to the "free" and ion pair, respectively.[14,27] The peak at about 635 cm^{-1} decreases in intensity with the increase of the phenolic concentration and nearly disappears when the phenolic concentration is at 15 phr. In the blend of PEO(100)/LiClO$_4$(25)/phenolic(15), the "free" fraction of ν(ClO$_4^-$) dominates over the fraction of ion pair, indicating that the lithium salt is nearly dissolved in the PEO(100)/LiClO$_4$(25)/phenolic(15) blend. However, the intensity of the ion pair peak increases drastically with a further increase of the phenolic concentration at 20 phr. The IR data on the ν(ClO$_4^-$) mode confirm that the addition of phenolic facilitates the ether group interacting with lithium ion, thus causing a reduction of the attractive force between cationic and anionic ions of the LiClO$_4$. However, the quantity of the ion pair increases when the addition of the phenolic is greater than 15 phr and this trend can be related to the strong interaction of hydrogen bonding as evidenced in the previous results (Fig. 6). The higher interaction of hydrogen bonding results in higher compaction between phenolic and PEO; thus the lithium salt is crowded out of this fully compatible system. From the IR results it can
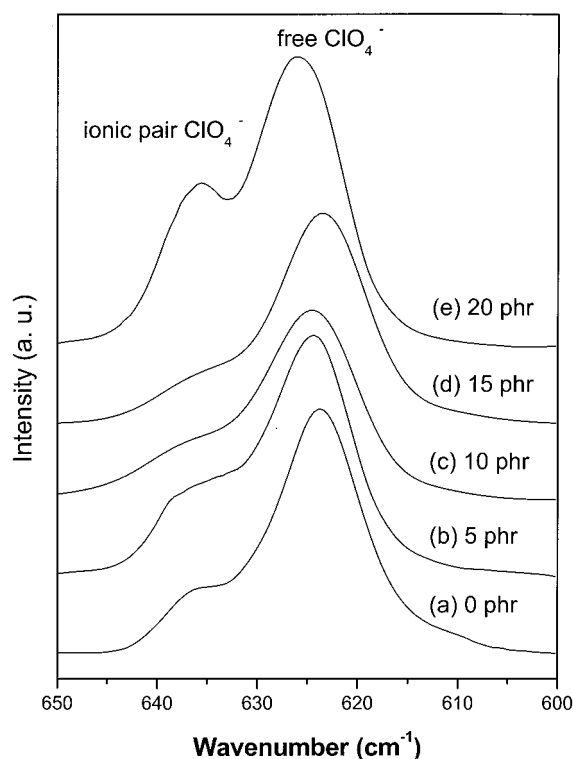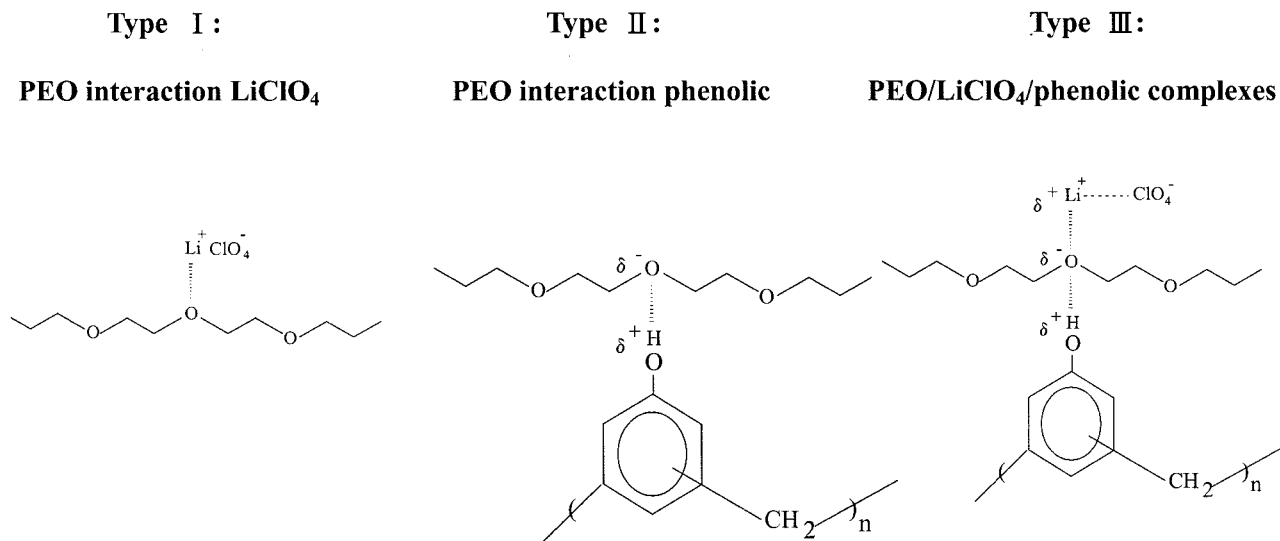

Figure 8 Infrared spectra in the 660–600 cm^{-1} region of PEO/LiClO$_4$/phenolic with various phenolic concentrations: (a) 100/25/0; (b) 100/25/5; (c) 100/25/10; (d) 100/25/15; (e) 100/25/20.

Type Ⅰ:

PEO interaction LiClO₄

Type Ⅱ:

PEO interaction phenolic

Type Ⅲ:

PEO/LiClO₄/phenolic complexes

Scheme 1 Three proposed types of ionic association of the PEO/LiClO₄/phenolic polymer electrolytes.

be concluded that the phenolic does not interact directly with the lithium salt, but the whole cationic charge environment is strongly influenced by the addition of phenolic resin in the PEO/LiClO₄/phenolic blend.

Based on the above findings on the microstructure of PEO/LiClO₄/phenolic polymer electrolytes, the total structural geometry is depicted in Scheme 1. The type I complex describes the solvated $Li^+ \cdots ClO_4^-$ ionic pair complexing with oxygen atom of PEO. The type II complex describes the hydrogen bonding between PEO and phenolic. The type III complex describes the intermolecular interaction of the PEO/LiClO₄/phenolic polymer electrolyte. This illustrates that the hydrogen bonding induced not only a positive charge on hydroxyl groups but also a negative charge on oxygen atoms of PEO. The electrons surrounding the ether oxygen were attracted by the higher electronegativity of the hydroxy group. The hydroxyl group of the phenolic plays the role of donating electrons in the hydrogen bonding system and induces the oxygen atom on PEO to become partially negative (type II complex). This induced, partially negative charge, on the oxygen atom will result in a stronger Lewis base. Furthermore, the lithium cation can be dissolved in the PEO/phenolic composite system, attributed to the strong Lewis base–acid interaction (type III complex). This induced, partially negative charge on the oxygen atom is also confirmed by the previous IR results (Fig. 6). Figure 6 indicates that the blend with 15 phr phenolic possesses the strongest ability to dissolve the LiClO₄, corresponding to the highest intensity of the "free" ion of $\nu(ClO_4^-)$. The optimum quantity of phenolic (15 phr) can also be related to the conductivity results shown in Figure 4. Therefore, it can be concluded that the addition of phenolic causes a change in

the charge environment of the oxygen atom of the PEO, which in turn induces a negative charge on the ether group and increases the quantity of "free" anions.

Dielectric property

It is well known that the addition of a plasticizer into a polymer matrix is able to increase its dielectric constant over that of the polymer host because the plasticizer facilitates the dissociation of ions and increases the number of effective charge carriers. The dielectric constant is of particular significance for ionic conducting polymers. Figure 9 presents the effect of phenolic concentration on the PEO dielectric constant at 27 and 40°C and constant frequency of 100 Hz. The curves in Figure 9 indicate that the dielectric constant increases with increasing phenolic concentration. The change in dielectric constant can be attributed to the partially negative charges induced by the hydrogen-bonding interaction. The blend containing a lower phenolic content induces fewer negative charges to orient in the direction of the applied field. Alternatively, for the blend with high phenolic content, a greater fraction of hydrogen bonding is able to induce more negative charges and results in a higher dielectric constant. Because of the higher mobility of the polymer matrix, a higher temperature also results in a higher dielectric constant of the composite, as would be expected.

⁷Li chemical shift of NMR spectra

For qualitative analysis of the lithium cation dynamics in the PEO/LiClO₄/phenolic composite electrolyte, measurements of the spin–lattice relaxation time T_1 of ⁷Li were carried out. The plot of the T_1 decay for the
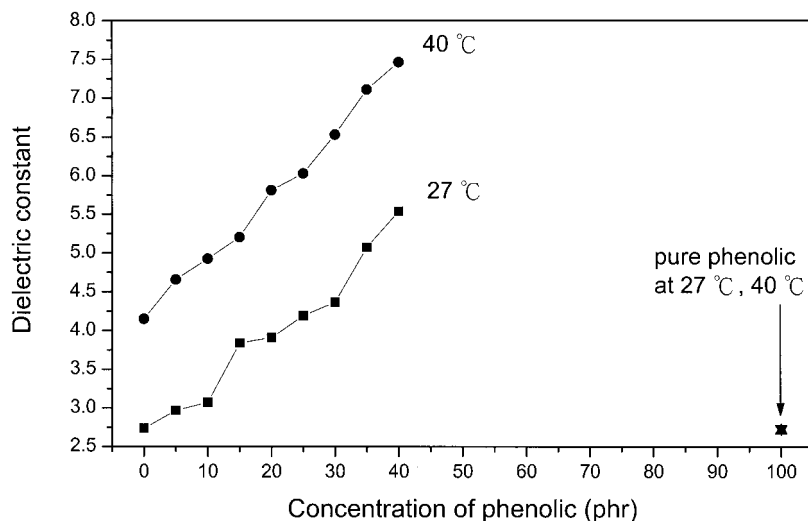
Figure 9 Dependency of dielectric constant of PEO(100)/phenolic with various concentrations of phenolic at the same temperature: (■) 27°C; (●) 40°C; (▲) pure phenolic at 27°C; (▼) pure phenolic at 40°C.

^{7}Li magnetization in the PEO/LiClO$_4$/phenolic as a function of phenolic content is shown in Figure 10. The addition of phenolic clearly gives higher mobility of the lithium cation, as shown by the gradually decreasing relaxation time values (T_1) for increasing phenolic concentration and the highest mobility is found at 15 phr phenolic. However, the T_1 increases with further increase of the phenolic content (20 phr). The increase of T_1 corresponds to the lower mobility of the lithium cation. This observed trend can be related to the formation of hydrogen bonding between phenolic and PEO. Earlier results indicated that the addition of phenolic is able to induce a negative charge on the ether group of PEO and causes stronger interaction

between the ether group and lithium cation. This induced negative charge on the ether group results in a strong Lewis base to dissolve the lithium salt more easily, and further disturbs the attractive force of the lithium salt, resulting in the higher mobility of lithium cation (lower T_1). From earlier results, in Figure 6, the increase in T_1 of lithium cation at PEO(100)/LiClO$_4$(25)/phenolic(20) can be attributed to the lithium salts being crowded out in this more compact system.

Thermal degradation analysis

A thermal gravimetric analyzer was used to carry out experiments on the weight loss and thermal decom-
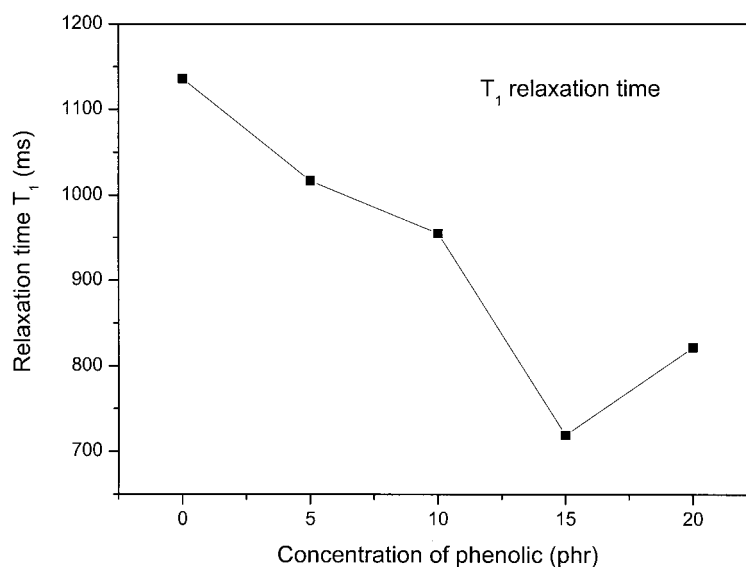

Figure 10 Relaxation time (T_1) scaled ^{7}Li CP/MAS NMR spectra of PEO(100)/LiClO$_4$(25)/phenolic with various phenolic contents.
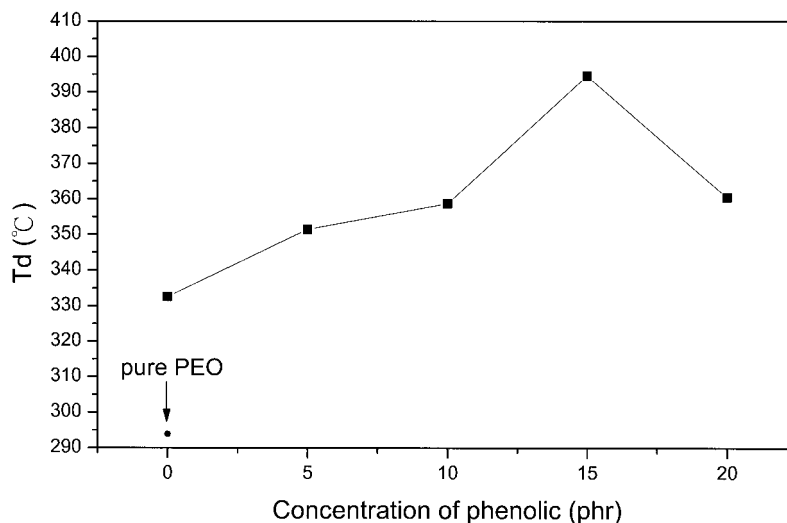
Figure 11 Thermal degradation temperature of PEO(100)/LiClO$_4$(25)/phenolic blends with various phenolic concentrations.

position behavior for PEO/LiClO$_4$/phenolic electrolytes. Figure 11 presents the thermal degradation temperature (T_d) of PEO(100)/LiClO$_4$(25)/phenolic blends as a function of phenolic concentrations. A similar trend was obtained: the T_d value increases with the increase in phenolic content and attains a maximum value when the phenolic concentration is at 15 phr. Subsequently, the T_d decreases with further increase in phenolic content. The T_d of the plain PEO is 294°C and that of pure phenolic is 591°C. With the incorporation of 25 phr LiClO$_4$ into PEO [PEO(100)/LiClO$_4$(25)], the T_d increases distinctly from 294 to 333°C. Such a change in thermal stability behavior can be attributed to the formation of a pseudo-crosslinked system by the interaction of PEO and lithium cation. With the addition of the phenolic concentration in the PEO(100)/LiClO$_4$(25)/phenolic blend, the T_d increases and reaches the maximum value (369°C) at 15 phr phenolic. However, with a further increase of the phenolic concentration (20 phr), a decrease in T_d (361°C) can be observed. The changes of T_d are strongly related to the interaction of hydrogen bonding attributed to the formation of pseudo-crosslinks between hydroxyl groups and ether groups. This trend of T_d is also consistent with conductivity, IR, and T_1 results.

CONCLUSIONS

This study demonstrated that the addition of an optimum content of phenolic is able to increase the ionic conductivity of the poly(ethylene oxide)-based electrolyte by about 2 orders of magnitude relative to the plain system. DSC, FTIR, DEA, and solid-state NMR studies indicate that hydrogen bonding is present between PEO and phenolic in the PEO/LiClO$_4$/phenolic composite electrolyte system. The phenolic does not directly interact with the lithium cation; on the contrary, the incorporation of the phenolic is able to induce a partial negative charge on the ether group of PEO by the strong hydrogen-bonding interaction between the hydroxyl group and the ether group. Furthermore, the ether group on PEO, possessing a stronger negative charge, is more effective in disturbing the attractive force between the lithium anion and cation and leads to the formation of a higher concentration of "free" anion and thus higher conductivity. This investigation demonstrated that the blend of PEO(100)/LiClO$_4$(25)/phenolic(15) possesses the highest ionic conductivity, attributed to the strongest hydrogen bonding interaction between PEO and phenolic. The optimum ionic conductivity was obtained from the balanced attractive forces among the oxygen atom of PEO, hydroxyl groups, and the lithium cation and anion.

References

1. Fenton, D. E.; Parker, J. M.; Wright, P. V. Polymer 1973, 3, 589.
2. Wright, P. V. Br Polym J 1975, 7, 319.
3. Armand, M. B. Solid State Ionics 1983, 9/10, 745.
4. Armand, M. B. Annu Rev Mater Sci 1986, 16, 245.
5. Scrosati, B. In: Polymer Electrolyte Reviews; MacCallum, J. R.; Vincent, C. A., Eds.; Elsevier Applied Science: New York, 1989; p. 315.
6. Scrosati, B. In: Applications of Electroactive Polymers; Scrosati, B., Ed.; Chapman & Hall: New York, 1993; p. 251.
7. Chao, S.; Wrighton, M. S. J Am Chem Soc 1987, 109, 2197.
8. Ratner, M. A.; Shriver, D. F. Chem Rev 1988, 88, 109.
9. Wang, L.; Yang, B.; Wang, X. L.; Tang, X. Z. J Appl Polym Sci 1999, 71, 1711.
10. Wang, X. L.; Li, H.; Tang, X. Z.; Chang, F. C. J Appl Polym Sci Polym Phys Ed 1999, 37, 837.
11. Skaarup, S.; West, K.; Zachan-Christiansen, B. Solid State Ionics 1988, 28–30, 975.

12. Plocharski, J.; Wieczorek, W. Solid State Ionics 1998, 28–30, 979.
13. Liquan, C. In: Materials for Solid State Batteries; Chowdari, B. V.; Radhakrishna, S., Eds.; World Scientific: Singapore, 1988; p. 69.
14. Quartarone, E.; Mustarelli, P.; Magistris, A. Solid State Ionics 1998, 110, 1.
15. Zhong, Z.; Guo, Q. Polymer 1998, 39, 517.
16. Penning, J. P., John, M. R. S. Macromolecules 1996, 29, 77.
17. Stotele, J. J.; Soldi, V.; Pires, A. T. N. Polymer 1997, 38, 1179.
18. Chu, P. P.; Wu, H.-D. Polymer 2000, 41, 101.
19. Wu, H. D.; Ma, C. C. M.; Li, M. S.; Su, Y. F.; Wu, Y. D. J Compos Part A: Appl Sci Manuf 1997, 28A, 895.
20. Wu, H. D.; Lee, C. T.; Ma, C. C. In: Proceedings of SAMPE Technical Conference, October 28, 1997, Orlando, FL; No. 29, 653.
21. Wu, H. D.; Chu, P. P.; Ma, C. C. M. Polymer 1997, 38, 5419.
22. Coleman, M. M.; Serman, C. J.; Painter, P. C. Macromolecules 1987, 20, 226.
23. Kim, H. I.; Pearce, E. M.; Kwei, T. K. Macromolecules 1989, 22, 3374.
24. Ennari, J.; Neelov, I.; Sundholm, F. Comput Theor Polym Sci 2000, 10, 403.
25. Lin-Vien, D.; Colthup, N. B.; Fately, W. G.; Grasselli, J. G. Infrared and Raman Characteristic Frequencies of Organic Molecules; Academic Press: San Diego, CA, 1991.
26. Pretsch; Clerc; Seibl; Simon. In: Table of Spectral Data for Structure Determination of Organic Compounds; Biemann, K., Ed.; Springer-Verlag: Berlin/Heidelberg/New York, 1983.
27. Nakanishi, K.; Solomon, P. H. Infrared Absorption Spectroscopy; K. N.: New York, 1976.
28. Coleman, M. M.; Graf, J. F.; Painter, P. C. Specific Interaction and Miscibility of Polymer Blends; Technomic: Lancaster, PA, 1991.
29. Purcell, K. F.; Drago, R. S. J Am Chem Soc 1968, 89, 2874.
30. Moskala, E. J.; Coleman, M. M. Polym Commun 1983, 24, 207.
31. Moskala, E. J.; Varnell, D. F.; Coleman, M. M. Polymer 1985, 26, 228.
32. Schantz, S. J Appl Phys 1988, 64, 2039.
33. Miller, A. G. J Phys Chem 1985, 89, 1193.
34. Frech, R. Electrochim Acta 1992, 37, 1499.
35. Dai, Y.; Greenbaum, S.; Golodnitsky, D.; Strauss, E.; Peled, E.; Rosenberg, Yu. Solid State Ionics 1998, 106, 25.
36. Chu, P. P.; Howard, J. J. Macromol Symp 1994, 86, 229.